

## Behaviour of Bi-material Interface Cracks in the Presence of Material Nonlinearity of Adherends

B. Dattaguru<sup>1</sup> and R. Muthukumar<sup>2</sup>

<sup>1</sup>Indian Institute of Science, Bangalore-560 012

<sup>2</sup>Vikram Sarabhai Space Centre, Trivandrum-695 547

### ABSTRACT

The well known features of crack face interpenetration/contact at the tip of an interface crack is re-examined using finite element analysis and assuming material nonlinear properties for the adherends. It was assumed in literature that the crack tips are fully open at all load levels in the presence of material nonlinearity of the adherends. Analysis for the case of remote tension shows that even in the presence of material nonlinearity, crack tip closes at small load levels and opens above a certain load level. Mixed-mode fracture parameters are evaluated for the situation when the crack tips are fully open. Due to the presence of nonlinearity, the mixed-mode fracture parameters are measured with the symmetric and anti-symmetric components of J-integral. The present analysis explains the sequence of events at the interface crack tip with progressively increasing remote tension load for the case of adherends with material nonlinear behaviour.

**Keywords:** Interface cracks, strain energy, finite element modelling, displacement profile, adherends, bi-materials, fracture behaviour

### 1. INTRODUCTION AND BASIC EQUATIONS

The fracture behaviour of bi-material interface cracks attracted considerable attention in the recent years. Literature<sup>1-5</sup> has shown that the order of singularity in bi-material interface crack is  $r^{(-0.5+\varepsilon)}$  where  $\varepsilon$  is the bi-material constant given by

$$\varepsilon = \frac{1}{2\pi} \log \left( \frac{1-\beta}{1+\beta} \right) \quad (1)$$

where  $\beta$  is a bi-material interface parameter proposed by Dundurs<sup>6</sup>.

The value of  $\beta$  is found to have values in the range of  $-0.5$  to  $+0.5$ . It will have a value of zero

for both materials having the same property or for materials with such a combination of properties to make  $\beta = 0$ . The  $\varepsilon$  will have values in the range of  $-0.175$  to  $+0.175$ . The complex singularity leads to oscillating displacement field and leads to the physically inadmissible interpenetration of crack faces, which was interpreted by researchers<sup>1-6</sup> as contact zone between the two faces of the crack at the bi-material interface.

The values for contact zone was expressed by Rice<sup>5</sup> as

$$r_{ct} = 2a \exp[-(\psi + \pi/2)/\varepsilon] \quad (2)$$

where  $a$  is the half crack length and  $\psi$  is the phase

angle of remote load ( $= 0$  when only remote tension is applied and  $= \pm \pi/2$  when only remote shear load is applied). The contact zone size is small for remote tension load but can not be ignored since the stress and displacement field around the crack tip plays a major role in the propagation characteristics. It is seen that the contact zone size can be as big as half the crack size for remote shear load case. It is also seen that the strain energy release rate (SERR) components will be oscillating due to the oscillating displacements. The SERR in tension will be zero even for remote tension load case with contact zone model since the crack face displacement is in pure shear mode and not in opening mode.

Most of the past studies assumed linear elastic behaviour of the materials. There were also limited studies which have considered nonlinearity of the materials<sup>7</sup>. While carrying out these studies, since the interest of the researchers was the stress field characterisation, the crack face interpenetration problem was not studied in detail. It was generally assumed that crack faces are fully open in the presence of material nonlinearity of the adherends. In the present study, considering the material nonlinear behaviour of the adherends, FEM analysis was conducted which demonstrates that the cracks do close at small load levels, and as the load is progressively increased, the crack tip opens. To study the fracture behaviour for the bi-material interface crack, J-integral was used in the presence of inelastic deformations. The SERR components in individual modes (mode-I and mode-II) were evaluated by splitting the stress and displacement fields into symmetric and anti-symmetric parts<sup>8</sup> and using the standard expressions for J-integral.

**2. TYPICAL CONFIGURATION AND FINITE ELEMENT MODEL**

Typical 2-D plane stress problem with interface crack is shown in Fig. 1. Domain (1) of material 1 is bonded to domain (2) of material 2, and a crack of length  $2a$  exists along the interface. The bond is assumed to be perfect so that the equilibrium and compatibility conditions are satisfied along the interface between the two materials where there is no crack. A finite width plate of  $2w$  width and

$2h$  height with  $a/w = 100$  and  $h/w = 1$  has been used in modelling. So, the model is for a large field compared to the crack size and it is subjected to remote tension loads. Only half of the plate was modelled simulating symmetry boundary conditions.

General purpose finite element software ANSYS was used for the analysis. To avoid the physically unacceptable crack face interpenetration, gap elements

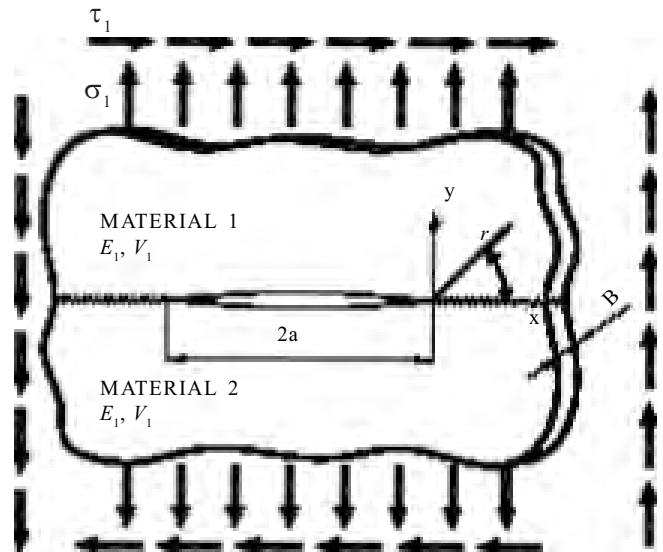


**Figure 1. Bi-material interface crack in an infinite plate with remote tension and shear loads.**

were used which allow crack opening but do not allow interpenetration and transfers direct compressive load in that case. Typical FEM mesh is shown in Fig. 2.

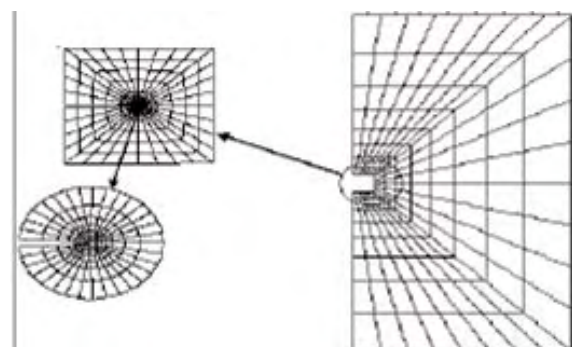


**Figure 2. Finite element model.**

**2.1 Material Model**

There are considerable difficulties to generate FEM solutions because in many situations the contact zone size is insignificantly small. For this purpose, Venkatesha<sup>7</sup>, *et al.* designed problems having large ratios of elastic properties of the adherends which leads to relatively large contact zone so that FEM analysis could be conducted with several nodes in the contact zone. In the present study, computations were carried out on large ratios of elastic properties (of the order of 10<sup>6</sup> for Young’s modulus and 49 for Poisson’s ratio) to start with, and by progressively decreasing the ratios of moduli to the order of 10 and the Poisson’s ratios to nearly equal which corresponds to practical situations. The material properties used are given in Table 1.

**Table 1. Elastic material properties**

Material set	$E_1$	$E_2$	$\nu_1$	$\nu_2$	$\beta$	$\varepsilon$	$r_d/a$
1	0.01	1e4	0.01	0.49	0.495	0.1727	2.25e-4
2	1.00	1e4	0.10	0.49	0.450	0.1543	7.56e-5
3	100.00	1e4	0.20	0.49	0.394	0.1324	1.41e-5
4	0.1e4	1e4	0.30	0.49	0.295	0.0968	1.79e-7

For analysing the elasto-plastic material, the incremental plasticity model with associated flow rule with von Mises yield criterion was used. An Euler backward scheme was used to enforce the consistency condition. The hardening rule uses Ramberg-Osgood stress-strain relationship given by

$$\varepsilon / \varepsilon_0 = \sigma / \sigma_0 + \alpha (\sigma / \sigma_0)^n \tag{3}$$

where  $\sigma_0$  and  $\varepsilon_0$  are the reference stress and strain which are taken to be uni-axial yield stress and strain respectively.  $\alpha$  is taken to be 0.1. The values of 1.5, 2, 3, 5 and 10 were used for the strain hardening exponent  $n$  to study the effect of strain hardening on the interpenetration/contact/crack opening. The form of stress-strain curves considered for analysis are shown in Fig. 3.

**3. LINEAR SOLUTIONS**

Linear analysis of the interface crack problem was conducted by several researchers in the past. Venkatesha<sup>9</sup> carried out linear analysis on interface

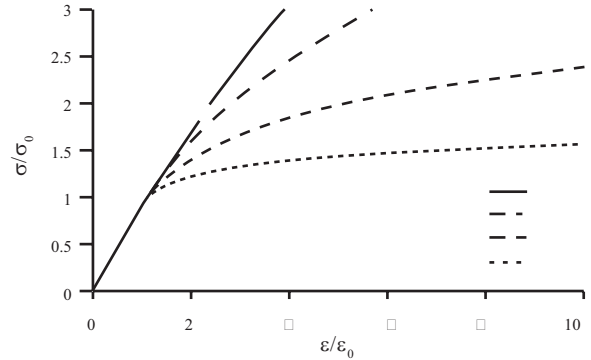


**Figure 3. Simulated stress–strain curve.**

problems with the material sets 1–4 used in the present study. Since the contact zone size was large for the case of these material sets, it was possible to conduct FEM analysis and visualise the contact zone.

In research works by Venkatesha<sup>9</sup>, *et al.* and Muthukumar<sup>10</sup>, such an analysis showed crack face interpenetration as shown in Fig. 4. The SERR components show oscillatory nature while these are evaluated using modified virtual crack closure integral (MVCCI) as the virtual crack extension tends to zero. This is shown in Fig. 5. This has been attributed to the inadmissible crack face interpenetration shown in Fig. 4. So, both<sup>9,10</sup> conducted FEM analysis using crack face contact conditions near the crack tip through gap elements in the software. The resulting displacement profile at the crack tip is shown in Fig. 6. There will be contact zone near the crack tip and mode-I SERR component will be zero. The condition at the crack tip will essentially be of mode-II.

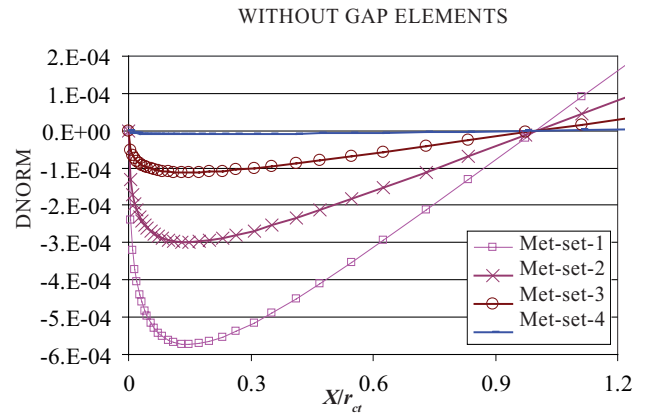


**Figure 4. Displacement profile – linear analysis without gap elements (interpenetration allowed).**

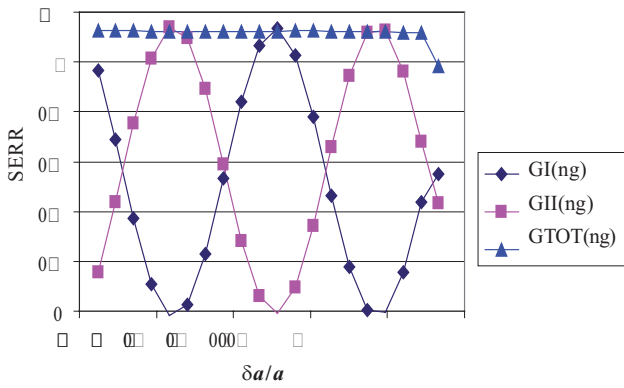


Figure 5. SERR (mode-I and mode-II) estimation from MVCCI; No gap elements used (interpenetration allowed).

Some of the researchers examined the phenomenon using realistic nonlinear properties of the adherends<sup>11</sup>. They came to a conclusion that crack faces are fully open in the presence of material nonlinear behaviour of the adherends. In the present study it was felt that there cannot be a discontinuous trend and so the problem was re-examined using FEM analysis. To make it possible to conduct FEM analysis, material sets proposed by Venkatesha<sup>9</sup> with large sized contact zones

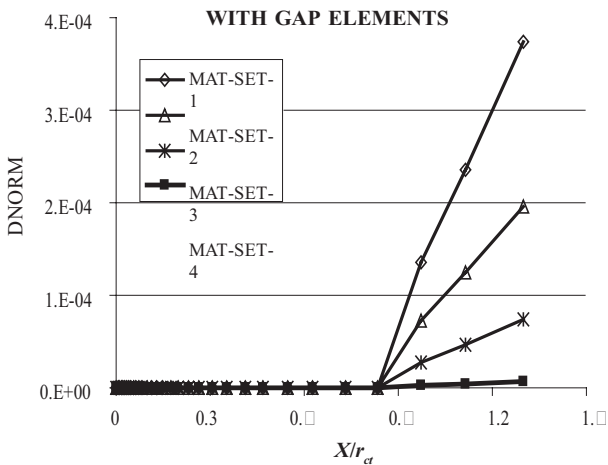


Figure 6. Displacement profile-linear analysis with gap elements (interpenetration not allowed).

were utilised. The MVCCI technique is not directly applicable for material nonlinear cases. So, the estimation of fracture parameters was carried out with J-integral. In mixed-mode problems, J-integral was used by splitting the stress field into

symmetric part to evaluate J-integral in opening mode and anti-symmetric part was used to evaluate J-integral in mode-II.

#### 4. SEPARATION OF COMPONENTS OF J-INTEGRAL

The method of separation of SERR components of mode-I and mode-II was proposed by Ishikawa<sup>8</sup>, *et al.* The method is explained below.

For separation of mode-I and mode-II components in a 2-D model, Ishikawa<sup>8</sup>, *et al.* suggested the method of separation of field variables into symmetric and anti-symmetric components which can then be used for calculation of mode-I and mode-II components of SERR. Let the two points  $P(x, y)$  and  $P'(x, -y)$  are assumed to be lying symmetric about the  $x$ -axis along which crack line is modelled. In a general case of arbitrary location of crack, local  $x$  and  $y$  axes can be defined to satisfy the above condition. The field variables at point  $P$  are  $s_{ij}$ ,  $e_{ij}$ ,  $u_i$ ,  $t_j$ , and at point  $P'$  the variables are  $s'_{ij}$ ,  $e'_{ij}$ ,  $u'_i$ ,  $t'_j$ . It was shown by Ishikawa<sup>8</sup>, *et al.* that the mode-I and mode-II components of field variables can be separated by the following equations:

$$\begin{Bmatrix} \sigma_{11}^I \\ \sigma_{22}^I \\ \sigma_{12}^I \end{Bmatrix} = \frac{1}{2} \begin{Bmatrix} \sigma_{11} + \sigma'_{11} \\ \sigma_{22} + \sigma'_{22} \\ \sigma_{12} - \sigma'_{12} \end{Bmatrix}, \quad \begin{Bmatrix} \sigma_{11}^{II} \\ \sigma_{22}^{II} \\ \sigma_{12}^{II} \end{Bmatrix} = \frac{1}{2} \begin{Bmatrix} \sigma_{11} - \sigma'_{11} \\ \sigma_{22} - \sigma'_{22} \\ \sigma_{12} + \sigma'_{12} \end{Bmatrix} \quad (4)$$

$$\begin{Bmatrix} \epsilon_{11}^I \\ \epsilon_{22}^I \\ \epsilon_{12}^I \end{Bmatrix} = \frac{1}{2} \begin{Bmatrix} \epsilon_{11} + \epsilon'_{11} \\ \epsilon_{22} + \epsilon'_{22} \\ \epsilon_{12} - \epsilon'_{12} \end{Bmatrix}, \quad \begin{Bmatrix} \epsilon_{11}^{II} \\ \epsilon_{22}^{II} \\ \epsilon_{12}^{II} \end{Bmatrix} = \frac{1}{2} \begin{Bmatrix} \epsilon_{11} - \epsilon'_{11} \\ \epsilon_{22} - \epsilon'_{22} \\ \epsilon_{12} + \epsilon'_{12} \end{Bmatrix} \quad (5)$$

$$\begin{Bmatrix} u_1^I \\ u_2^I \end{Bmatrix} = \frac{1}{2} \begin{Bmatrix} u_1 + u'_1 \\ u_2 - u'_2 \end{Bmatrix}, \quad \begin{Bmatrix} u_1^{II} \\ u_2^{II} \end{Bmatrix} = \frac{1}{2} \begin{Bmatrix} u_1 - u'_1 \\ u_2 + u'_2 \end{Bmatrix} \quad (6)$$

From Eqns (4) to (6), and simplifying the equations due to symmetry of the geometry with  $x$ -axis (crack line), the J-integral for mode-I and mode-II can be written as

$$J = \sum_{i=1}^N \left\{ \begin{array}{l} \frac{1}{2} \left[ \sigma_{xx}^I \sigma_{yy}^I \sigma_{xy}^I \right] \begin{bmatrix} \epsilon_{xx}^I \\ \epsilon_{yy}^I \\ \epsilon_{xy}^I \end{bmatrix} n_x - \left[ \sigma_{xx}^I \sigma_{yy}^I \sigma_{xy}^I \right] \\ \left[ \begin{array}{cc} n_x & 0 \\ 0 & n_y \\ n_y & n_x \end{array} \right] \begin{bmatrix} \frac{\partial u_x^I}{\partial x} \\ \frac{\partial u_y^I}{\partial x} \end{bmatrix} \end{array} \right\} d\Gamma$$

$$+ \sum_{i=1}^N \left\{ \begin{array}{l} \frac{1}{2} \left[ \sigma_{xx}^{II} \sigma_{yy}^{II} \sigma_{xy}^{II} \right] \begin{bmatrix} \epsilon_{xx}^{II} \\ \epsilon_{yy}^{II} \\ \epsilon_{xy}^{II} \end{bmatrix} n_x - \left[ \sigma_{xx}^{II} \sigma_{yy}^{II} \sigma_{xy}^{II} \right] \\ \left[ \begin{array}{cc} n_x & 0 \\ 0 & n_y \\ n_y & n_x \end{array} \right] \begin{bmatrix} \frac{\partial u_x^{II}}{\partial x} \\ \frac{\partial u_y^{II}}{\partial x} \end{bmatrix} \end{array} \right\} d\Gamma \quad (7)$$

= J<sub>I</sub> + J<sub>II</sub>

From the FE results, the contours were selected along the integration points in a path around the crack and the J-integrals were calculated. This method has been used for estimation of mode-I and mode-II components of SERR in an elastic bi-material interface crack.

**5. DISPLACEMENT SOLUTIONS WITH MATERIAL NONLINEARITY**

The displacement results from both linear and nonlinear analyses are normalised as shown in Eqn (8). This equation is adapted from the elastic displacement solution provided by Rice<sup>5</sup>.

$$D_{norm} = \frac{u_y}{\frac{(1 + \kappa_1)}{\mu_1} + \frac{(1 + \kappa_2)}{\mu_2}} \quad (8)$$

The displacement profiles from the elasto-plastic analysis for various levels of loads (as percentage of yield strength) for the material set-1 with n = 2, and n=10 are presented in Figs 7–8. Also the displacement profiles for material set-4 for exponent n=10 are shown in Fig. 9.

It is seen from Figs 7–9 that the stress levels at which the crack tips fully open decrease as n tends to be large. Obviously, the load at which the crack tip fully opens is infinitely large when n tends to 1 implying elastic behaviour of adherends. These are cross-plotted at a later time to bring in

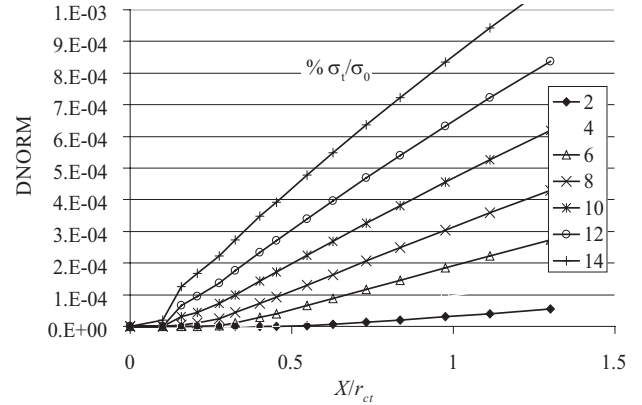


Figure 7. Displacement profile-nonlinear analysis material set-1, n = 2.

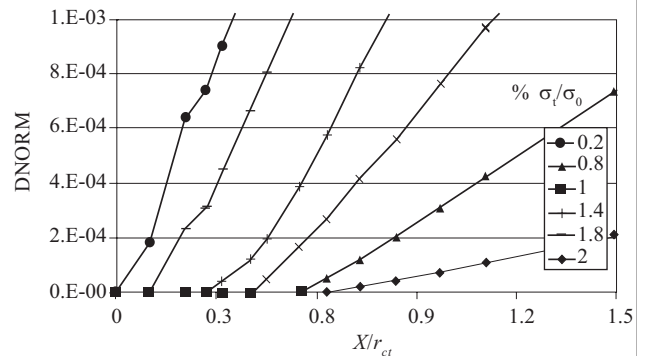


Figure 8. Displacement profile-nonlinear analysis material set 1, n = 10.

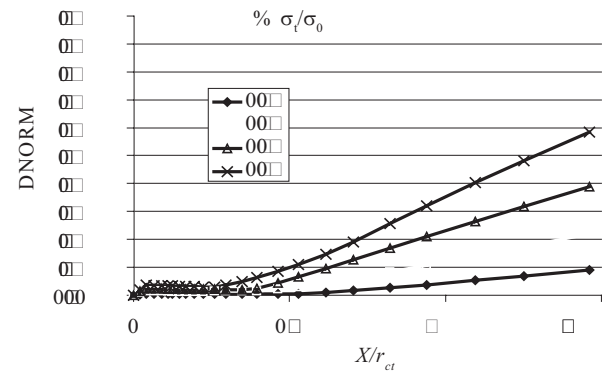


Figure 9. Displacement profile-nonlinear analysis material set-4, n = 10.

the effects of these parameters. The extent of contact zone with load level is plotted for all the material sets in Figs 10-13. The figures also show the effect of  $n$  on the contact zone size. It is seen that as  $n$  tends to the large value of 10 used in the current analysis, the load level required for any contact zone size decreases. As  $n$  tends to 1, which is the elastic case, the load level required for any contact zone size increases.

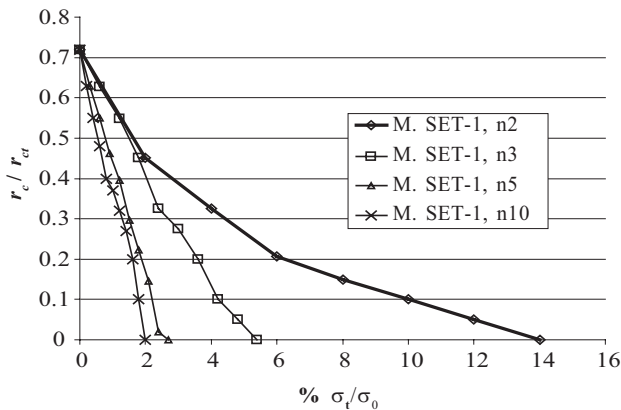


Figure 10. Contact zone size as a function of load (material set-1).

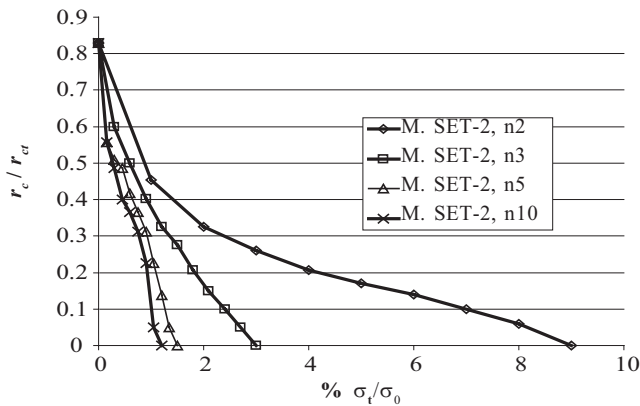


Figure 11. Contact zone size as a function of load (material set-2).

From the displacement profiles it is seen that the crack tips do close at small load levels, and as the remote tension is increased, the crack tips open confirming the fact observed by several that the interface crack tips do open in the presence of material nonlinearity. However, the present study shows that they do open above certain load levels and this load level is dependent on the type of stress-strain curve and the bi-material constant. The load level at which the crack tips fully open increases with decreasing

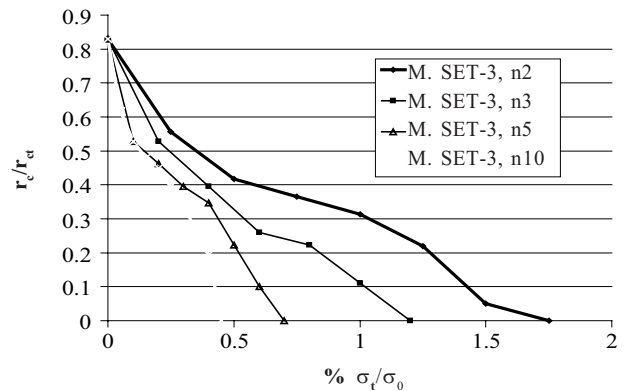


Figure 12. Contact zone size as a function of load (material set-3).

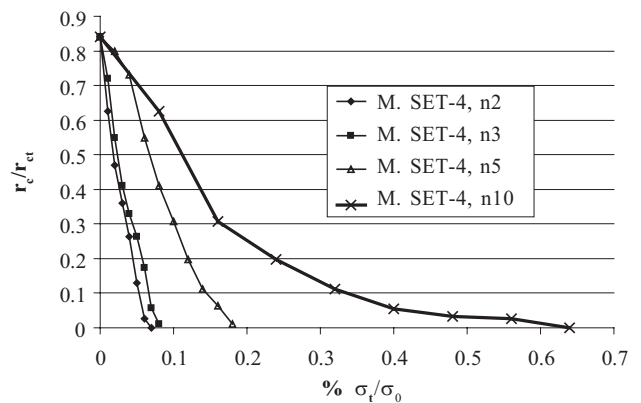


Figure 13. Contact zone size as a function of load (material set-4).

exponent. The same load levels for which the crack tips are fully open increases with increasing bi-material constant. This shows that as the modular ratio of the dissimilar adherends increases, the crack tips remain closed for higher values of  $\epsilon$  ratio.

Figure 14 gives the minimum remote tension load (as ratio of yield strength in %) required for complete opening of crack as a function of the strain-hardening exponent  $n$ . The minimum load required for fully open crack is designated as  $(\sigma_t/\sigma_0)^*$  in the figure. As expected, the load level  $(\sigma_t/\sigma_0)^*$  to open the crack asymptotically increases to infinity as  $n$  tends to 1, which is the elastic case.

In Fig. 15, the  $(\sigma_t/\sigma_0)^*$  is plotted as the variation of the bi-material parameter  $\epsilon$ . It is clearly seen that the load requirement for the crack to open reduces to less than 1 per cent of yield strength when  $\epsilon$  is around or less than 0.1. But if the value

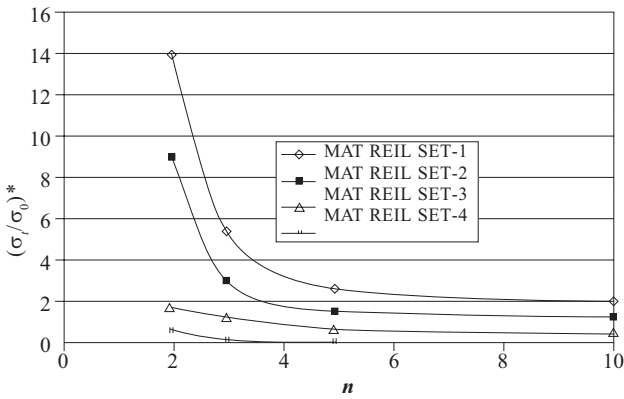


Figure 14. Load level for crack opening as function of  $n$ .

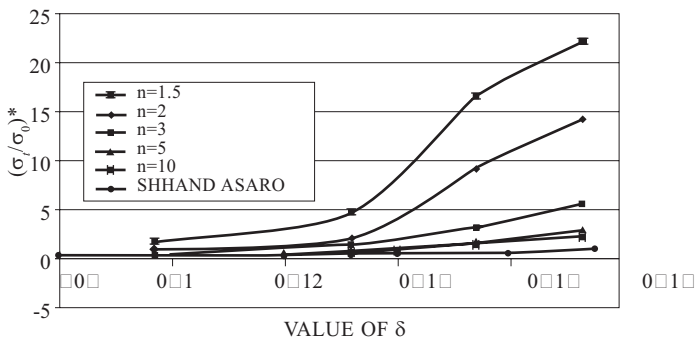


Figure 15. Load level for crack opening as function of  $\epsilon$ .

of  $\epsilon$  is around the upper limit of 0.175, minimum load requirement is as high as 22 per cent of yield strength for a crack to be fully open with  $n = 1.5$ . This could be much larger for  $1 \leq n \leq 1.5$ .

In this plot, the result of Shih and Asaro<sup>7</sup> is also presented. They have also given the results from finite element analysis with  $n$  varying from 3 to 10. But they appear to have concluded that the results are independent of strain-hardening coefficient  $n$ , as against the findings in this paper which show dependence on  $n$ .

### 6. MODE-MIXITY IN PRESENCE OF MATERIAL NONLINEARITY

The mode-mixity in the presence of material nonlinearity can be characterised by estimation and study of  $J$  in mode-I and mode-II. Figure 16 shows the components of  $J$ -integral for material set-1 at a low load level such as 1 per cent of yield strength and at a large load level of 50 per cent of yield strength. At 1 per cent of yield strength,

there is a crack face contact zone of  $x/r_{ct} \approx 0.3$ . For this case, the mode-I and mode-II components of  $J$  show oscillatory behaviour and finally for value of  $r$  less than the contact zone, there is mode-II dominance. At higher loads, the crack tip opens fully, causing mode-I value to increase.

Similar results are obtained for material sets 2, 3, and 4, and in all the cases when load level is large, the crack fully opens, the  $J$  components obtained as  $J(r)$  with  $r \rightarrow 0$  show non-zero values for both mode-I and mode-II components. The mode-mixity as obtained from the components of  $J$  for very small values of  $r/a$  are shown in Fig. 17. The figure shows mode-I component of  $J$  as a fraction of  $J$  total. At small values of load,  $J$  in mode-I is zero due to crack closing and at large values of load levels when crack fully opens, one could see mode-I and mode-II components to be significant.

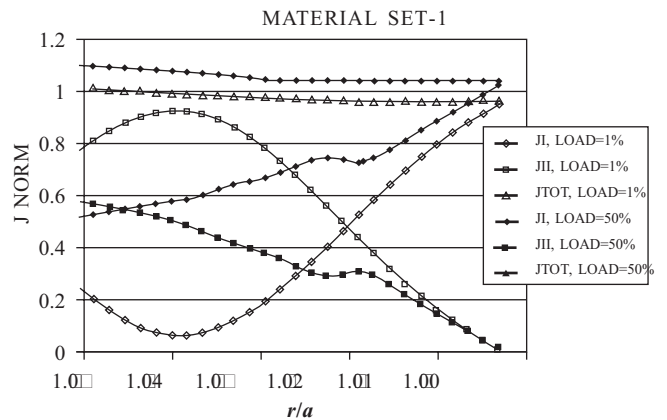


Figure 16.  $J_I$  and  $J_{II}$  values for material set-1,  $n = 10$ .

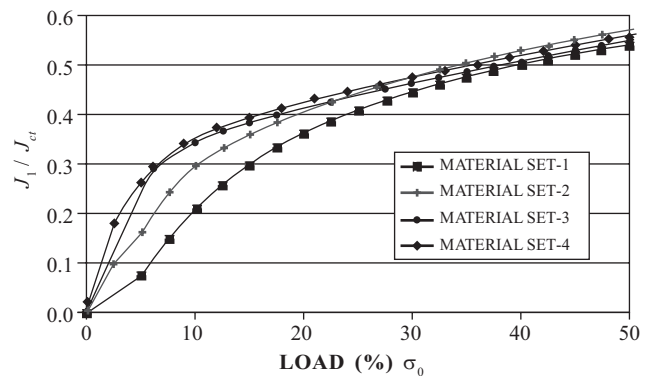


Figure 17.  $J_I$  and  $J_{II}$  as variation of remote load.

## 7. CONCLUSIONS

Finite element analysis of bi-material interface crack problem was carried out to understand the effect of nonlinear material properties on the contact zone ( $r_c$ ). For this purpose, a specially designed problem, where the materials across the interface have large ratio of elastic properties, was selected so that the contact zone size is large. Finite element model could place several nodes within this contact zone and a parametric study could be made on the effect of ratio of elastic properties and plasticity hardening exponent  $n$  on the contact zone size. The following conclusions are drawn:

- The classical problem of displacement oscillations near crack tip and interpenetration could be reproduced in linear FE analysis with good accuracy.
- With gap elements to avoid interpenetration, the contact length was found to be less than the case allowing interpenetration.
- With crack tip plasticity effects, the interpenetration and displacement oscillations were found to be vanishing for remote tension loads of up to 14 per cent of yield strength ( $\sigma_0$ ).
- The load level  $(\sigma_t/\sigma_0)^*$  at which the crack fully opens is found to be dependent on the elastic bi-material parameter  $\varepsilon$  and plastic hardening exponent  $n$ .  $(\sigma_t/\sigma_0)^*$  decreases with decrease in  $\varepsilon$  ratio and also decreases with increasing value of  $n$ .
- $(\sigma_t/\sigma_0)^*$  was found to be independent of yield strength of materials.

## REFERENCES

1. Williams, M.L. The stresses around a fault or crack in dissimilar media. *Bull. Seismological Soc. Amer.*, 1959, **49**, 199-04.
2. Comninou, M. The interface crack. *Trans. ASME, J. Appl. Mech.*, 1977, **44**, 631-36.
3. Comninou, M. Interface cracks with friction in contact zone. *Trans. ASME, J. Appl. Mech.*, 1977, **44**, 780-81.
4. Comninou, M. The interface crack in a shear field. *Trans. ASME, J. Appl. Mech.*, 1978, **45**, 287-90.
5. Rice, J.R. Elastic fracture mechanics concepts for interfacial cracks. *Trans. ASME, J. Appl. Mech.*, 1988, **55**, 98-103.
6. Dundurs, J. Edge bonded dissimilar orthogonal elastic wedges under normal and shear loading. *Trans. ASME, J. Appl. Mech.*, 1969, **36**, 650-52.
7. Shih, C.F. & Asaro, R.J. Elastic-plastic and asymptotic fields of interface cracks. *Int. J. Fracture*, 1990, **42**, 101-16.
8. Ishikawa, H.; Kitagawa, H. & Okamura, H. J-integral of a mixed mode crack and its application. *In Proceedings of 3<sup>rd</sup> International Conference on Mechanical Behaviour of Materials*. Vol. 3, Pergamon, Oxford, 1980, 447-55.
9. Venkatesha, K.S.; Dattaguru, B. & Ramamurthy, T.S. Finite element analysis of an interface crack with large crack tip contact zones. *Engg. Fracture Mech.*, 1996, **54**, 847-60.
10. Muthukumar, R. Effect of material nonlinearity of adherends on fracture behaviour of bi-material interface cracks. Department of Aerospace Engineering, Indian Institute of Science, Bangalore. PhD thesis.
11. Raju, I.S.; Crews, J.H. (Jr.) & Amnipour, M.A. Convergence of strain energy release rate components for edge delaminated composite laminates. *Engg. Fracture Mech.*, 1988, **30**, 383-96.

## Contributors



**Prof B. Dattaguru** obtained his BE (Electrical Technol), ME (Aeronautics), and PhD(Engg) from the Indian Institute of Science (IISc), Bangalore. He is former Chairman of the Department of Aerospace Engineering, Chairman of Centre for Scientific and Industrial Consultancy, and Convenor for the Joint Advanced Technology Programme at IISc, Bangalore. He held KSIIDC Chair for three years and received *Rustom Choksi Award* for excellence in engineering research from IISc, Bangalore; *Academic Excellence Award 2002* from DRDO; and *Padma Shree, (2005)*. His fields of interest are: Aerospace structures, composite materials, fracture mechanics and finite element methods. He retired from IISc, Bangalore in 2004 and is currently a Consultant to M/s Satyam Computers, M/s Cades Digitech, M/s CSM Software at Bangalore.



**Dr R. Muthukumar** received his ME from Department of Mechanical Engineering and PhD (Nonlinear Fracture Mechanics), IISc, Bangalore. He is working in Indian Space Research Organization for the past 23 years in the field of design, analysis, and development of aerospace structures. Currently, he is the Head, Liquid Propellant Systems Centre, Trivandrum. His areas of specialisation are: Aerospace structural design, nonlinear structural analysis, and fracture mechanics.